© 2017. Published by The Company of Biologists Ltd | Journal of Experimental Biology (2017) 220, 2554-2562 doi:10.1242/jeb.157792

RESEARCH ARTICLE

Hindlimb muscle function in turtles: is novel skeletal design correlated with novel muscle function?

Christopher J. Mayerl[1,*], Jenna E. Pruett[2], Morgan N. Summerlin[1], Angela R. V. Rivera[3] and Richard W. Blob[1]

ABSTRACT

Variations in musculoskeletal lever systems have formed an important foundation for predictions about the diversity of muscle function and organismal performance. Changes in the structure of lever systems may be coupled with changes in muscle use and give rise to novel muscle functions. The two extant turtle lineages, cryptodires and pleurodires, exhibit differences in hindlimb structure. Cryptodires possess the ancestral musculoskeletal morphology, with most hip muscles originating on the pelvic girdle, which is not fused to the shell. In contrast, pleurodires exhibit a derived morphology, in which fusion of the pelvic girdle to the shell has resulted in shifts in the origin of most hip muscles onto the interior of the shell. To test how variation in muscle arrangement might influence muscle function during different locomotor behaviors, we combined measurements of muscle leverage in five major hindlimb muscles with data on muscle use and hindlimb kinematics during swimming and walking in representative semiaquatic cryptodire (*Trachemys scripta*) and pleurodire (*Emydura subglobosa*) species. We found substantial differences in muscle leverage between the two species. Additionally, we found that there were extensive differences in muscle use in both species, especially while walking, with some pleurodire muscles exhibiting novel functions associated with their derived musculoskeletal lever system. However, the two species shared similar overall kinematic profiles within each environment. Our results suggest that changes in limb lever systems may relate to changes in limb muscle motor patterns and kinematics, but that other factors must also contribute to differences in muscle activity and limb kinematics between these taxa.

KEY WORDS: Locomotion, Biomechanics, Leverage, EMG, Turtle

INTRODUCTION

Differences in structure across animal species are often used as a basis for predicting differences in their function (Hulsey et al., 2008; Anderson and Patek, 2015). One of the most common sources of structural variation that has been examined in this context is the leverage of muscle systems (Smith and Savage, 1956; Biewener, 1989; Westneat, 1994; Kargo and Rome, 2002). The leverage of muscles about joints can be compared through the measurement of moment arms, which are defined as the shortest distance between the line of action of a muscle–tendon complex and the center of rotation of a joint about which the complex acts (Vogel, 2013). Muscles with larger moment arms generate a greater moment about a joint for a given level of input force, reducing the absolute amount of force that the muscle must generate to balance an external load (Hutchinson et al., 2005). Yet, in addition to structural features, muscle function is also determined by a wide range of dynamic components (Roberts et al., 1997; Ahn and Full, 2002), including the timing of muscle activity (Biewener and Gillis, 1999; Gillis and Blob, 2001). Thus, correlations between changes in leverage and activity timing could profoundly affect the functional roles of muscles throughout the evolution of a lineage (Lauder and Reilly, 1996). However, it is unclear whether such correlations should be expected, given that remarkably similar patterns of muscle activity have been documented for both locomotor and feeding behaviors across taxa that exhibit highly divergent structures (e.g. Jenkins and Goslow, 1983; Wainwright and Lauder, 1986; Westneat and Wainwright, 1989; Dial et al., 1991).

Structural variations in the locomotor systems of turtles provide an opportunity to specifically test for associations between changes in muscle leverage and changes in muscle activation patterns. The two major lineages of turtles, cryptodires and pleurodires, show differences in pelvic girdle structure that are correlated with differences in the origins of many hindlimb muscles. Cryptodires possess the ancestral configuration, in which the pelvis can move relative to the shell (Walker, 1973; Mayerl et al., 2016). In contrast, pleurodires exhibit a derived condition, in which the pelvis has been fused to the shell and become immobile (Walker, 1973; Mayerl et al., 2016). These skeletal changes are associated with many of the muscles responsible for controlling the hindlimb shifting from origins on the pelvis in cryptodires to origins on the interior surface of the shell in pleurodires (Fig. 1, Fig. S1; Walker, 1973). Because the moment arm of a muscle is strongly influenced by the location of its origin, these structural rearrangements of the pelvic girdle in pleurodires are likely to substantially change the leverage of the muscles that control hindlimb motion. Despite these differences in their anatomical structure, most freshwater turtles of both lineages show broadly similar patterns of hindlimb motion (e.g. using sprawling limb posture on land and rowing strokes in the water: Zug, 1971; Blob et al., 2008; Mayerl et al., 2016). Thus, changes in muscle leverage may not be reflected in their patterns of action. Alternatively, it is possible that the two lineages might activate their limb muscles differently but, with differences in muscle leverage, those activity patterns could lead to similar locomotor movements.

To investigate whether changes in limb muscle leverage are correlated with changes in muscle activity in turtles, we (1) compared the leverage of five major hindlimb muscles between representative semiaquatic cryptodire (*Trachemys scripta*) and pleurodire (*Emydura subglobosa*) species, and (2) used electromyography (EMG) to measure the activity patterns of these muscles while (3) recording hindlimb kinematics during swimming and walking. We found that changes in muscle leverage may contribute to novel muscle use in pleurodires, but that some

[1]Department of Biological Sciences, Clemson University, Clemson, SC 29634, USA. [2]Department of Biological Sciences, Auburn University, Auburn, AL 36849 USA. [3]Department of Biology, Creighton University, Omaha, NE 68178, USA.

*Author for correspondence (cmayerl@clemson.edu)

C.J.M., 0000-0003-0402-8388

Received 6 February 2017; Accepted 2 May 2017

Journal of Experimental Biology

Journal of Experimental Biology (2017) 220, 2554-2562 doi:10.1242/jeb.157792

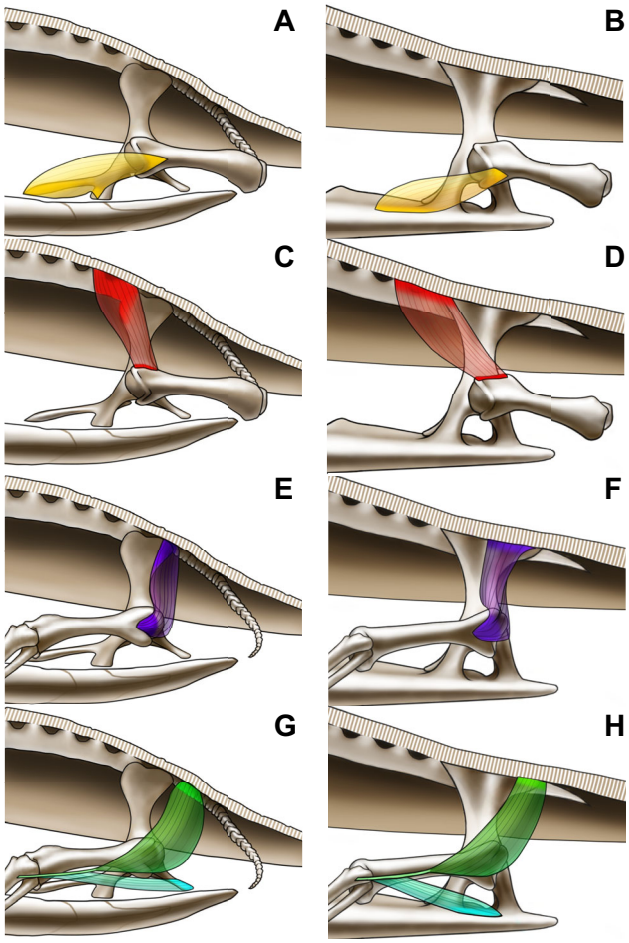

Fig. 1. Isolated hindlimb muscles of turtles that have experienced a change in their location of origin associated with pelvic girdle fusion in the pleurodire lineage. Muscles have shifted from the ancestral origin on the pelvis in cryptodires (left, *Trachemys scripta*) to the shell in pleurodires (right, *Emydura subglobosa*). (A,B) Puboischiofemoralis internus (PIFI, yellow); (C,D) iliofemoralis (ILF, red); (E,F) caudi-iliofemoralis (CIF, purple); (G,H) flexor tibialis interus (FTI, green). Darker shading represents locations of muscle origin and insertion. The femorotibialis (FT) is not illustrated because it does not cross the hip and is thus not directly affected by pelvic girdle fusion.

pleurodire limb muscles show novel patterns of activity even without changes to their anatomical leverage. Additionally, our results indicate that hindlimb kinematics differ strongly between locomotor environments (i.e. water versus land) in both turtle lineages, but that cryptodires and pleurodires may utilize similar kinematics in each environment through different patterns of muscle use.

MATERIALS AND METHODS

Experimental animals

Six adult Jardine River turtles (16.5–22.3 cm), *Emydura subglobosa* (Krefft 1876), were purchased from a commercial supplier (Turtles and Tortoises, Brooksville, FL, USA). Three adult red-eared sliders (18.5–19.5 cm), *Trachemys scripta* (Shoepff 1792), were collected with hoop traps from a spillway of Lake Hartwell, Pickens County, SC, USA (South Carolina Scientific Collection permit 28-2016). We also supplemented our cryptodire data with results from two additional individuals that were published in a previous study (Blob et al., 2008). Turtles were housed in pairs in 600-liter stock tanks equipped with pond filters, a submerged 200 W heater (maintaining water at 25°C) and dry basking platforms. Tanks were located in a temperature-controlled greenhouse facility, exposing turtles to ambient light patterns throughout the course of experiments (February 2015 to August 2016). Turtles were fed a diet of commercial pellets (ReptoMin, Tetra, Blacksburg, VA, USA), supplemented with earthworms. All animal care and experimental procedures were approved by the Institutional Animal Care and Use Committee at Clemson University (protocols 2013–051, 2014–079).

Collection and analysis of muscle properties

Although our measurements of muscle structure were the last chronological stage in our study, we will describe these methods first because their results provide the primary context for interpreting our data on muscle activity patterns and limb movements. At the conclusion of data collection for muscle use and kinematic patterns, experimental animals were euthanized and the muscles of the right (non-instrumented) hindlimb were dissected to determine their moment arms and physiological cross-sectional areas (PCSA). Focus muscles included the puboischiofemoralis internus (PIFI; Fig. 1A,B), iliofemoralis (ILF; Fig. 1C,D), femorotibialis (FT; Fig. S2), dorsal and ventral heads of the flexor tibialis internus (FTI-D and FTI-V; Fig. 1E,F), and caudi-iliofemoralis (CIF; Fig. 1G,H). The FTI is characterized by possessing a dorsal head, which originates on the sacral vertebrae in both lineages, and a smaller ventral head, which originates on the puboischiadic ligament and the border of the ischium in cryptodires, but originates on the plastron in pleurodires (Walker, 1973). Because of these differences, we collected moment arm data on both heads of this muscle separately, although we were not able to collect motor pattern data from the ventral head. Based on the anatomical locations of these five muscles and previous studies of cryptodire turtles, the PIFI and ILF are considered the primary hip protractors, FT is regarded as a knee extensor, FTI is considered a hip retractor and knee flexor, and CIF is considered a hip retractor (Walker, 1973; Blob et al., 2008; Aiello et al., 2013).

Muscle measurements were collected from all six *E. subglobosa* used to collect muscle activity and kinematic data, as well as from six previously euthanized *T. scripta* that had been frozen after earlier experiments (Rivera and Blob, 2010). To identify the joint center of rotation, we palpated and manipulated the leg and placed a metal pin at the center of rotation of the hip. We then observed the location of the pin to ensure that no translation occurred as the limb was manipulated. To quantify the moment arm of a muscle about a joint, we used digital calipers to measure the perpendicular distance from the joint to the midline of each focus muscle spanning the joint in the directions of hip abduction/adduction, hip protraction/retraction and knee flexion/extension, as applicable. Moment arms for the hip were measured with the limb parallel with the plane of the plastron at 45, 90 and 135 deg of protraction/retraction, relative to the cranial axis of the body. For flexion and extension of the knee, we measured moment arms at maximal flexion and extension, as well as when the crus was positioned perpendicular to the thigh. These measurements represented the moment arms of each muscle throughout a complete limb cycle. For each muscle, we then used the average of the three measurements for each variable in statistical analyses. To compare hindlimb muscle leverage across differently sized individuals and provide a better reflection of muscle mechanical advantage at joints, we converted our moment arm measurements into size-normalized moment arms by dividing the moment arm by thigh length for moments occurring at the hip, and by crus length for moments occurring at the knee.

Journal of Experimental Biology (2017) 220, 2554-2562 doi:10.1242/jeb.157792

After joint moment arms were measured, muscles were dissected out from each turtle. Muscle fascicle lengths were determined by measuring the length of fascicles at the center of the muscle when the muscle was laid flat on the dissecting tray, and muscles were weighed using a digital scale. PCSA was calculated following standard protocols (Biewener and Full, 1992). To account for minor differences in size across individual turtles, PCSA was normalized for comparisons by dividing raw PCSA by the square of the length of the thigh.

Collection and analysis of EMG data

EMG data were collected from five focal hindlimb muscles (PIFI, ILF, FT, FTI-D and CIF). These muscles are thought to be the primary muscles used to power hindlimb movements in turtles, are the largest muscles in the hindlimb and cover all major planes of hindlimb motion during locomotion (Walker, 1973; Blob et al., 2008). Additionally, limited data for these muscles have been collected from cryptodire turtles in previous experiments (Blob et al., 2008; Aiello et al., 2013), providing comparisons with our new recordings. Data were collected during both swimming and terrestrial walking behaviors in a custom-built, recirculating flow tank. For aquatic trials, turtles were induced to swim by adjusting flow speed to elicit constant swimming behavior against flow (Pace et al., 2001). In walking trials, turtles were filmed walking over a clear Plexiglas platform into a water-filled refuge. As in previous work, a transparent surface was required to collect kinematic data, but the dried Plexiglas surface did not inhibit terrestrial locomotion (Rivera and Blob, 2010). For each turtle, 25–30 limb cycles were collected for each locomotor behavior.

To ensure accurate placement of electrodes, we performed dissections on previously euthanized individuals in order to determine external landmarks for EMG implantation. Prior to implantation, we induced analgesia and anesthesia with intramuscular injections of 1 mg kg^{-1} butorphenol, 30 mg kg^{-1} ketamine and 1 mg kg^{-1} xylazine into the right forelimb, following published procedures (Rivera and Blob, 2010; Rivera et al., 2011). While anesthetized, anatomical landmarks were marked for kinematic measurements (see below), and bipolar fine-wire electrodes (0.05 mm diameter, insulated stainless steel; 0.5 mm barbs; California Fine Wire Co., Grover Beach, CA, USA) were implanted percutaneously into target muscles in the left hindlimb using hypodermic needles. For each experiment, up to 15 implants were performed, with target muscles receiving between two and four electrodes to ensure successful recordings even if some electrodes failed. Electrode wires were glued together into two cables, with wires inserted into posterior muscles (CIF and FTI-D) being grouped into one cable, and wires inserted into anterior muscles (PIFI, ILF and FT) grouped into the other cable. These cables were given several centimeters slack, and were then secured to the carapace with waterproof tape. Turtles were then allowed to recover from anesthesia overnight.

During locomotor trials, EMG signals were relayed from electrodes in turtles to a Grass 15LT amplifier system (West Warwick, RI, USA) for amplification (10,000 times) and filtering (60 Hz notch filter, 30 Hz–6 kHz bandpass). Analog EMG signals were converted to digital data and collected at 5000 Hz using custom LabVIEW software (v.6.1; National Instruments, Austin, TX, USA) routines. Following data collection, turtles were euthanized by an intraperitoneal injection of sodium pentobarbital (200 mg kg^{-1}) and experimental limbs were dissected to verify electrode placement.

EMG data were synchronized with limb kinematics by triggering a signal generator that simultaneously produced a square wave in the EMG data and a light pulse visible in the video. EMGs were then analyzed using custom LabVIEW software routines to identify bursts of muscle activity. The variables calculated included the percentage of the cycle at which muscle activity began (onset) and ended (offset). The number of trials from which EMG data were collected varied across individuals and muscles because of differences in electrode implant success.

Collection and analysis of kinematic data

Coincident with EMG data collection, kinematic data were collected at 100 Hz using two digitally synchronized high-speed video cameras (Phantom V5.1, Vision Research, Wayne, NJ, USA). Lateral and ventral views were collected simultaneously, with the ventral view obtained by directing the camera at a mirror angled at 45 deg with respect to the transparent bottom of the flow tank arena.

To facilitate measurement of kinematics, anatomical landmarks (13 ventral, nine lateral) were marked with non-toxic white nail polish, with a smaller, black point painted in the center of the white dot to create trackable, high-contrast points (Fig. 2). The landmarks used in both views included: tip of the nose, hip, knee, ankle, digits 1, 3 and 5, and anterior and posterior points on the bridge of the shell. We also marked points on the right, left, anterior and posterior margin of the plastron that were visible in ventral view. Landmarks were tracked using DLTDataViewer5 (Hedrick, 2008), and the resulting three-dimensional coordinate data were processed using custom MATLAB routines to determine kinematic excursions during swimming and walking (Rivera and Blob, 2010). Kinematic data included femoral protraction and retraction angles, femoral elevation and depression angles, extension and flexion angles of the knee and ankle, and the rotation (feathering) angle of the pes. These variables were then processed through a quintic spline to smooth and interpolate the data to 101 values, representing 0–100% of the limb cycle (0 being a fully protracted limb). These procedures

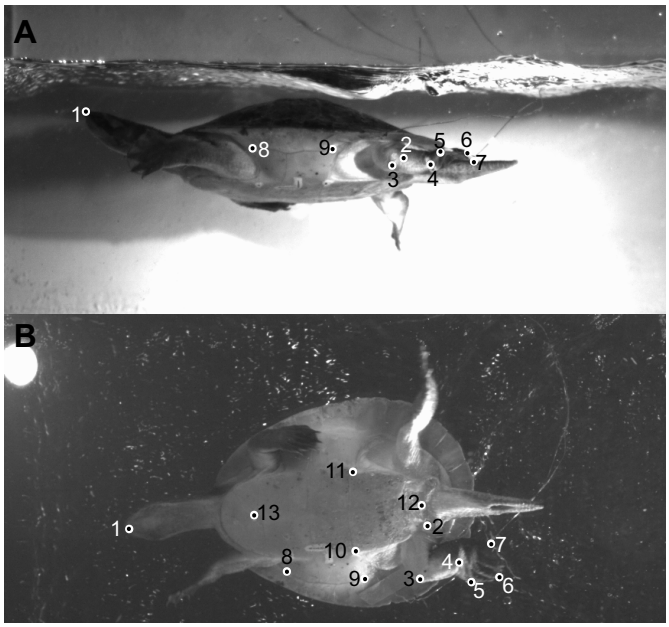

Fig. 2. Representative still images showing landmarks digitized for kinematic analysis. (A) Lateral view; (B) ventral view. Points 1–9 are the same in both views; points 10–13 are only visible in ventral view. Landmarks: 1, tip of nose; 2, hip; 3, knee; 4, ankle; 5, digit 1; 6, digit 3; 7, digit 5; 8, anterior point on bridge; 9, posterior point on bridge; 10, point on left side of plastron; 11, point on right side of plastron; 12, posterior point on plastron; 13, anterior point on plastron.

Journal of Experimental Biology

Journal of Experimental Biology (2017) 220, 2554-2562 doi:10.1242/jeb.157792

facilitated comparisons of kinematic profiles for locomotor cycles of different absolute durations.

Kinematic angles were defined as follows. A femoral protraction/retraction angle of 0 deg indicates a femur perpendicular to the midline of the body, where positive values indicate a more protracted femur and negative values indicate greater retraction. A femoral elevation/depression angle of 0 deg indicates the femur is in the horizontal plane of the turtle, where positive angles indicate elevation and negative angles indicate depression. A knee extension/flexion angle of 0 deg indicates a fully flexed knee, whereas a 180 deg angle indicates a fully extended knee. An ankle angle of 0 deg indicates the pes was dorsiflexed to fold on top of the distal crus, whereas an angle of 90 deg indicates that the pes was held perpendicular to the crus, and an angle of 180 deg indicates that the pes was parallel to and extending from the distal crus. Pes rotation (feathering) angle was calculated as the angle between a vector pointing along the anteroposterior midline and a vector emerging from the plantar surface of the pes, which was defined by the points marking the ankle and the tips of digits 1 and 5. This angle was transformed by subtracting 90 deg from each value (Pace et al., 2001). A high drag orientation of the pes, with the paddle directed perpendicular to the direction of travel, is indicated by an angle of 90 deg, whereas a low drag orientation of the pes is indicated by an angle of 0 deg.

Statistical analysis

Unless otherwise noted, all statistical analyses were performed in R (v 3.2.1, www.r-project.org).

Muscle anatomy

Anatomical properties for the muscles we measured from both turtle lineages, including size-normalized moment arm for each direction of motion for each muscle, as well as size-normalized PCSA, were compared using Cohen's *d* tests (effsize; R package version 0.7.0, https://CRAN.R-project.org/package=effsize), which evaluate the difference between two means divided by the standard deviation of the data (Cohen, 1992). This provides an effect size estimate of the treatments (in this case, the difference between the two species). We considered any variables with a Cohen's *d* of greater than 1 to be different between the two lineages, a conservative estimate for considering large effect sizes (Cohen, 1992).

EMGs

We performed a canonical discriminant analysis (CDA) using onset and offset timings for each muscle in each environment to determine the primary variables explaining the variation between species and environments (MASS; Venables and Ripley, 2002). A Wilks' lambda test was performed to determine whether the differences explained by the discriminant variables were significant. Because of electrode and equipment failures, we do not have data for every muscle from each individual. Data included in the analysis were mean muscle onset and offset timings of each muscle in each species (Table S1).

Kinematics

Differences in kinematics between environments and species were compared using a CDA (MASS; Venables and Ripley, 2002). Variables included in the CDA were maximal protraction and retraction angles, maximum abduction and adduction angles, maximum knee flexion and extension angles, maximum ankle flexion and extension angles, and maximum and minimum pedal feathering angles. A Wilks' lambda test was performed to determine whether the differences explained by the discriminant variables were significant.

We further used linear mixed effects models for each set of kinematics (lmer4; Bates et al., 2015) to test for differences between species within an environment. We used species as a fixed effect, and individual and trial (intercept varying within trial) as random effects [X~species+(1|individual/trial)]. *P*-values were obtained by likelihood ratio tests of the full model with the effect in question against the model without the effect in question. Effect sizes based on mixed effects models were calculated following published methods (Cohen, 1992; Xu, 2003).

RESULTS

Muscle leverage and size

We found that muscles that showed no change in origin between the two lineages (FT and FTI-D; Fig. 1, Fig. S2) showed no difference in size-normalized moment arm for any moment (Table 1). In

Table 1. Differences between cryptodire and pleurodire turtles in normalized muscle physiological cross-sectional areas (PCSA) and size-normalized moment arm (MA) for directions of hindlimb motion

Muscle	Variable	Cryptodire	Pleurodire	Cohen's *d*
PIFI	PCSA	$7.55\times10^{-8}\pm3.63\times10^{-9}$	$7.59\times10^{-8}\pm1.19\times10^{-8}$	=
	MA-Pro/ret	0.145±0.012	0.188±0.015	+
	MA-Ab/add	0.057±0.005	0.150±0.030	+
ILF	PCSA	$4.21\times10^{-8}\pm5.72\times10^{-9}$	$5.33\times10^{-8}\pm1.19\times10^{-8}$	=
	MA-Pro/ret	0.131±0.011	0.173±0.029	=
	MA-Ab/add	0.127±0.022	0.273±0.028	+
FT	PCSA	$3.66\times10^{-8}\pm3.11\times10^{-9}$	$4.98\times10^{-8}\pm9.62\times10^{-9}$	=
	MA-Flex/extend	0.121±0.021	0.106±0.007	=
FTI-D	PCSA	$3.92\times10^{-8}\pm4.29\times10^{-9}$	$5.43\times10^{-8}\pm7.34\times10^{-9}$	=
	MA-Pro/ret	0.278±0.025	0.271±0.017	=
	MA-Ab/add	0.100±0.016	0.119±0.011	=
	MA-Flex/extend	0.169±0.025	0.156±0.013	=
FTI-V	PCSA	$1.75\times10^{-5}\pm3.48\times10^{-6}$	$5.23\times10^{-5}\pm4.13\times10^{-6}$	=
	MA-Pro/ret	0.103±0.009	0.112±0.011	=
	MA-Ab/add	0.108±0.007	0.189±0.028	+
	MA-Flex/extend	0.139±0.186	0.187±0.022	+
CIF	PCSA	$6.93\times10^{-8}\pm5.74\times10^{-6}$	$6.23\times10^{-8}\pm9.93\times10^{-9}$	=
	MA-Pro/ret	$0.204\pm1.43\times10^{-6}$	0.317±0.052	+
	MA-Ab/add	0.077±0.021	0.237±0.039	+

Values reported are means±s.e. (PCSA in m^2, MA is dimensionless, N=6 cryptodires, 6 pleurodires). =, two lineages statistically equivalent; +, pleurodire mean greater than cryptodire (Cohen's d>1). PIFI, puboischiofemoralis internus; ILF, iliofemoralis; FT, femorotibialis; FTI, flexor tibialis internus; CIF, caudi-iliofemoralis.

Journal of Experimental Biology (2017) 220, 2554-2562 doi:10.1242/jeb.157792

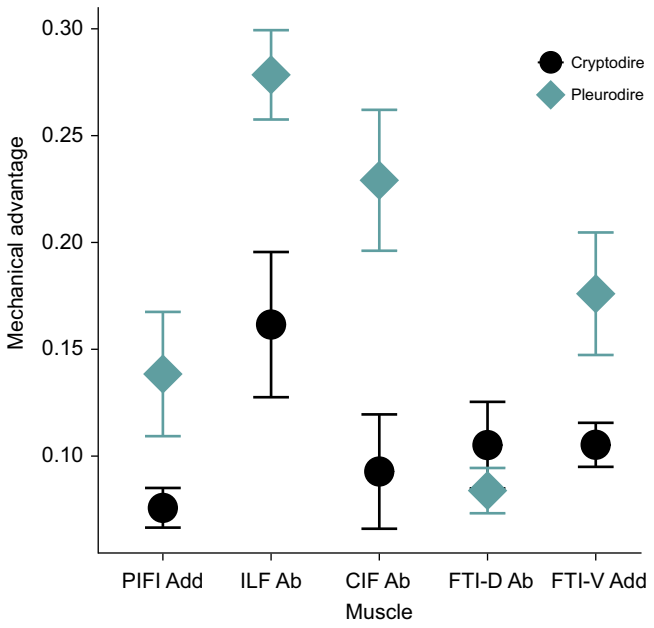

Fig. 3. Size-normalized moment arms in ab/adduction for the five focal hindlimb muscles for each species. The femorotibialis (FT) is not plotted because it does not exert moments about the hip. PIFI Add, puboischiofemoralis internus adduction; ILF Ab, iliofemoralis abduction; CIF Ab, caudi-iliofemoralis abduction; FTI-D Ab, flexor tibialis internus (dorsal head) abduction; FTI-V Add, flexor tibialis internus (ventral head) adduction. For all muscles that have experienced a shift in origination (all but FTI-D), the pleurodire exhibits greater ab/adduction than the cryptodire. Black circles, cryptodire (*Trachemys scripta*, *N*=6 individuals); blue diamonds, pleurodire (*Emydura subglobosa*, *N*=6 individuals).

contrast, the other four muscles (PIFI, ILF, FTI-V and CIF; Fig. 1) all showed greater size-normalized moment arms in abduction/adduction in pleurodires than they did in cryptodires (Table 1, Fig. 3). When normalized by thigh length, PCSA was similar between lineages for all muscles. We found very few changes in size-normalized moment arms for protraction/retraction or flexion/extension, although size-normalized moment arms for protraction in PIFI and retraction in CIF were larger in pleurodires than cryptodires (Table 1).

Muscle activity patterns

In each lineage, we found substantial differences in muscle activity between swimming and walking (Fig. 4, Table S2). Comparing patterns within each environment between the lineages, the specific timings of onset and offset differ in some muscles during swimming, but they are active during the same general periods of activity in both cryptodires and pleurodires (Fig. 4A). In contrast, during walking, larger differences are exhibited between the lineages, with substantial changes in activity timing for most muscles, and generally increased duration of activity in pleurodires (Fig. 4B). Pleurodires exhibit bursts of activity during both stance and swing for FT that are similar to the two burst patterns for this muscle found in cryptodires (Blob et al., 2008). However, pleurodires also exhibited an unexpected second burst of activity by PIFI during the stance phase of walking that has not been observed in walking cryptodires (Fig. 4B).

CDA identified two axes of variation that together explained 98.02% of variation in EMG patterns between species and across environments (Fig. 5). Canonical 1 (C1, 75.01% of variation) separated pleurodire walking motor patterns from all other motor patterns. Walking pleurodires were particularly distinguished by later offset timing of CIF, FTI and ILF, as well as later onset timing of PIFI (Table S2). Canonical 2 (C2, 23.01% of variation) separated pleurodire swimming from cryptodire walking and swimming. Pleurodire swimming was characterized primarily by later offset of FT (Table 2). A Wilks' lambda test indicated that the differences explained by the discriminant variables were significant (Wilks' lambda=0.007, $P<0.001$).

Kinematics

We found no differences in velocity [in body lengths (BL) per second] between the two species during swimming (*T. scripta*: 1.59 ±0.02 BL s^{-1}, *E. subglobosa*: 1.57±0.02 BL s^{-1}, $P=0.547$, Cohen's $d=0.141$, $\Omega^2=0.396$) or walking (*T. scripta*: 0.53±0.04 BL s^{-1}, *E. subglobosa*: 0.47±0.02 BL s^{-1}, $P=0.987$, Cohen's $d=0.207$, $\Omega^2=0.253$). The two species spent similar amounts of time during thrust and recovery while swimming, with both lineages shifting from retraction to protraction at roughly 45% of the limb cycle. However, while walking, cryptodires began femoral protraction at approximately 61% of the cycle, whereas pleurodires did not begin femoral protraction until 73% of the cycle (Fig. 6).

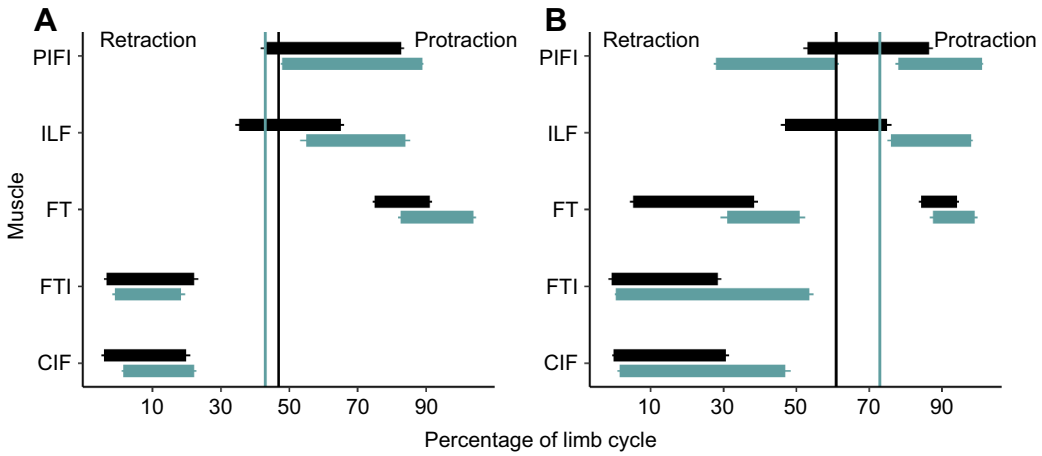

Fig. 4. Hindlimb muscle use while swimming and walking in cryptodire (*T. scripta*) (black) and pleurodire (*E. subglobosa*) (blue) turtles. (A) Swimming; (B) walking. Bars represent the mean and standard error for the period of activity for each muscle. Vertical lines indicate the switch from retraction to protraction for each lineage for each behavior. See Table S1 for sample sizes for each muscle in each habitat for each species.

Journal of Experimental Biology

Journal of Experimental Biology (2017) 220, 2554-2562 doi:10.1242/jeb.157792

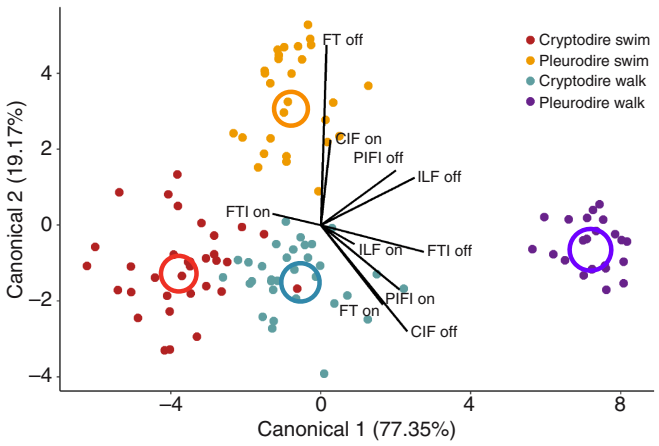

Fig. 5. Canonical discriminant function analysis of hindlimb muscle activity patterns in cryptodire (*T. scripta*) and pleurodire (*E. subglobosa*) turtles. Muscle use is defined primarily by species, with walking pleurodires showing the most distinct patterns along the first axis (Canonical 1), and swimming pleurodires showing the most distinct patterns along the second axis (Canonical 2). Colors of points indicate different cycle categories: red, cryptodire swimming (*N*=33); yellow, pleurodire swimming (*N*=28); light blue, cryptodire walking (*N*=32); purple, pleurodire walking (*N*=23). Colored rings represent the 95% confidence limit for the mean of each of these three groups. Black lines indicate the magnitude and direction of the loading of each variable (Youngerman et al., 2014). Pleurodire walking (Canonical 1) differentiated from the other three groups, and is represented primarily by delayed offset of CIF, FTI and ILF, as well as delayed onset of PIFI. Canonical 2 discriminates pleurodire swimming from cryptodire walking and swimming, and is loaded most strongly by later onset of CIF (caudi-iliofemoralis), and later offset of FT (femorotibialis). See Table 2 for loadings.

In addition to differences in the timing of limb movements, pleurodires and cryptodires also differed in the extent of limb movement. In both swimming and walking, cryptodires protracted their femur to a greater degree than pleurodires, but retracted them less (Fig. 6, Table S3). Cryptodires also depressed their femur less than pleurodires, and extended their knee less (Fig. 6, Table S1). There was little difference in ankle extension or flexion between the two lineages in either environment (Fig. 6, Table S1). However, during swimming, pleurodires orient the paddle of their pes in a higher drag position than cryptodires during thrust (Fig. 6, Table S1).

CDA identified two primary axes that together explained 97.41% of variation in hindlimb kinematics between species and across environments. C1 (87.98% of variance) was defined primarily by differences between walking and swimming, whereas C2 (9.43% of variance) distinguished cryptodires from pleurodires (Fig. 7). Walking cycles were characterized by positive scores on C1, reflecting larger protraction angles, decreased knee flexion and decreased pes rotation (during swing). Swimming cycles were characterized by negative scores on C1, reflecting increased pes rotation angle (foot oriented in 'high drag' position, occurring during thrust). Thus, during swimming, there is greater movement in the distal elements of the hindlimb as the animal produces drag-based propulsion, whereas during walking, the limb is protracted further to extend the stride. On C2, pleurodires are distinguished by decreased knee flexion and increased ankle extension. A Wilks' lambda test indicated that the differences explained by the discriminant variables were significant (Wilks' lambda=0.16, P<0.001).

DISCUSSION

The fusion of the pelvis to the shell in pleurodire turtles has resulted in derived locations of origin for muscles that power their hindlimb movements (Walker, 1973). These shifts in muscle origin have resulted in pleurodires exhibiting greater size-normalized moment arms for femoral adduction and abduction in these muscles when compared with cryptodire turtles (Table 1). We found that some muscles that exhibit drastic changes in muscle leverage between these lineages show changes in motor pattern, especially while walking. Additionally, some muscles that show little anatomical difference between the two lineages can also show differences in hindlimb muscle use during locomotion. Thus, pelvic girdle fusion and the subsequent muscular reorganization of the hindlimb muscles may account for some differences in limb function between cryptodire and pleurodire turtles, but other dynamic components of muscle function likely also contribute to differences in limb muscle use between these lineages (Roberts et al., 1997; Ahn and Full, 2002).

In pleurodires, all muscles that have experienced a shift in origin also demonstrate greater size-normalized moment arms for ab/adduction. This change in leverage does not appear to influence muscle use during swimming for the semiaquatic turtle species we studied, as both lineages exhibited similar patterns of muscle activity in water (Fig. 4A). However, when these turtles moved on

Table 2. Muscle activity patterns during locomotion while swimming and walking in cryptodire and pleurodire turtles

		Swim		Walk			
Muscle	Action	Cryptodire	Pleurodire	Cryptodire	Pleurodire	Canon 1	Canon 2
PIFI	On	43.08±1.38	48.35±0.45	53.12±1.22	77.96±0.73	0.41	−0.26
	Off	82.80±0.83	89.23±0.27	86.53±1.01	101.76±0.32	0.40	0.30
ILF	On	35.37±1.21	55.18±1.76	46.83±1.20	76.57±0.99	0.14	−0.07
	Off	65.09±1.07	84.11±1.52	74.83±1.27	98.35±0.47	0.46	0.29
FT	On			5.24±0.97	31.87±1.85		
Stance	Off			38.54±1.01	51.58±1.43		
FT	On	75.05±0.74	82.58±0.75	84.18±0.60	87.59±0.82	0.33	−0.39
Swing	Off	91.25±0.65	104.02±0.72	93.95±0.60	99.62±0.26	0.06	0.97
FTI	On	−3.38±0.74	−0.96±0.66	−0.71±0.86	0.49±0.36	−0.22	0.05
	Off	22.29±1.21	18.43±1.13	28.50±0.93	53.60±1.16	0.54	−0.12
CIF	On	−4.23±0.73	1.82±0.50	−0.14±0.39	1.50±0.60	0.07	0.46
	Off	19.94±1.26	22.27±0.61	30.73±0.89	47.35±1.48	0.41	−0.48

Values are mean±s.e. activity timing (in percentage of limb cycle, 0 being a fully protracted limb). Canonical values are loaded scores for each variable in the CDA. PIFI, puboischiofemoralis internus; ILF, iliofemoralis; FT, femorotibialis; FTI, flexor tibialis internus; CIF, caudi-iliofemoralis.

Journal of Experimental Biology (2017) 220, 2554-2562 doi:10.1242/jeb.157792

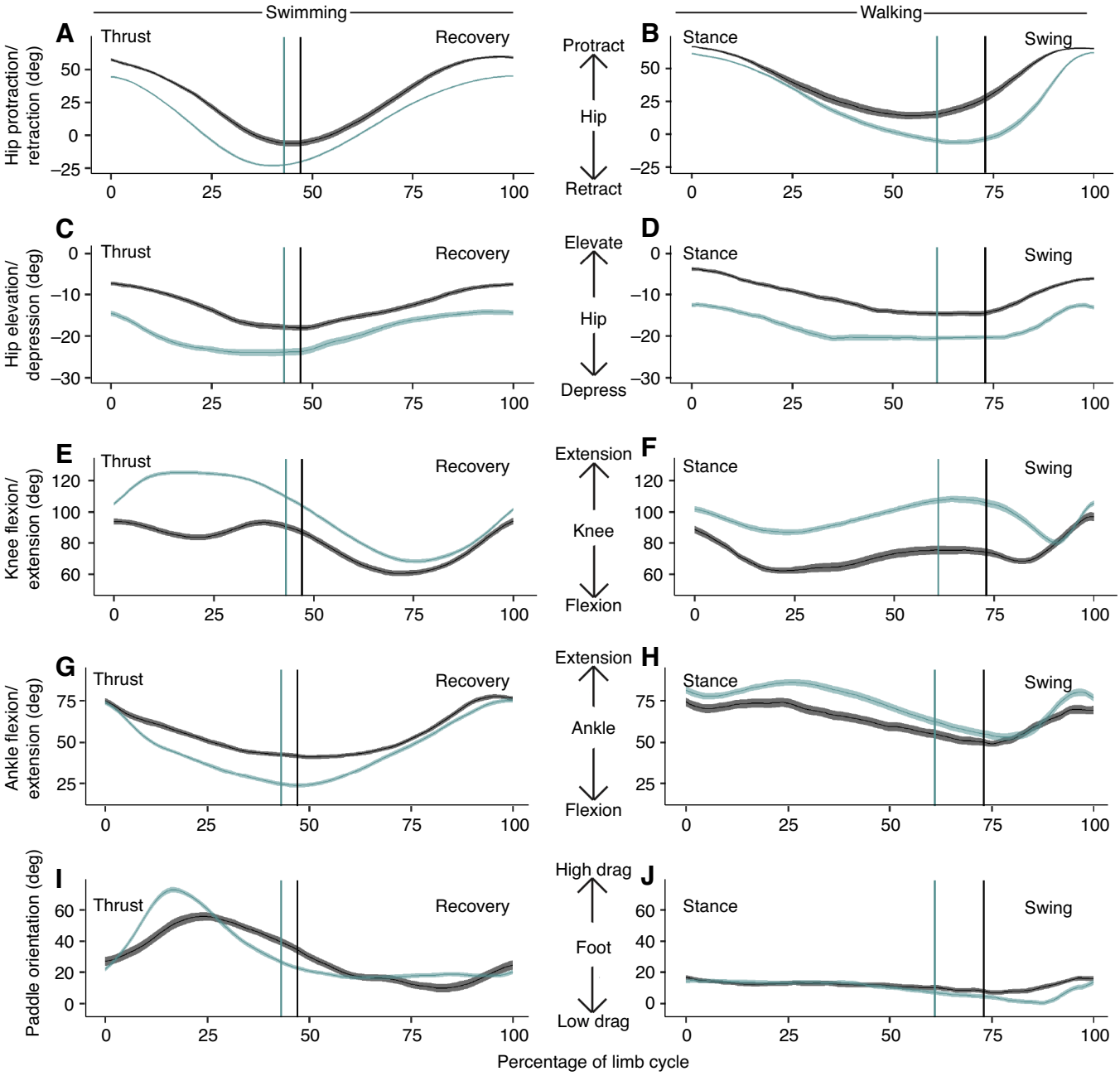

Fig. 6. Mean hindlimb kinematics of cryptodire (*T. scripta*, black) and pleurodire (*E. subglobosa*, blue) turtles while swimming (left, cryptodire: *N*=5 individuals, 84 cycles; pleurodire: *N*=6 individuals, 149 cycles) and walking (right, cryptodire: *N*=5 individuals, 88 cycles; pleurodire: *N*=6 individuals, 116 cycles). (A,B) Hip protraction/retraction; (C,D) hip elevation/depression; (E,F) knee flexion/extension; (G,H) ankle flexion/extension; (I,J) paddle orientation. Solid lines indicate the mean value throughout the limb cycle, with shaded areas indicating standard error of the mean throughout the limb cycle.

land, we observed substantial differences in muscle use between the taxa (Fig. 4B). In some cases, the shifts in leverage owing to girdle fusion may contribute to novel functional capacities for specific muscles. For example, PIFI is typically regarded as a femoral protractor in cryptodires (Walker, 1973; Blob et al., 2008). However, PIFI has approximately triple the size-normalized moment arm for adduction in pleurodires than cryptodires, and shows a novel burst of activity during the femoral retraction (stance) phase of walking in pleurodires, during which femoral adduction is greater than in cryptodires (Fig. 6D). This burst of muscle activity in PIFI corresponds with a delayed onset of the hip retractor CIF during pleurodire walking (Fig. 4B). In CIF, the pleurodire size-normalized moment arm for abduction was also over triple what was observed in cryptodires (Table 1). Thus, we see substantial changes in leverage in these two muscles, which also show drastic differences in muscle activity between the two lineages while walking. The novel burst of activity in PIFI could potentially be functioning to counteract the increased duration of CIF activity, supporting the body during stance as the limb is retracted.

Although some differences in hindlimb motor patterns and kinematics between pleurodires and cryptodires, like those for PIFI,

Journal of Experimental Biology

Journal of Experimental Biology (2017) 220, 2554-2562 doi:10.1242/jeb.157792

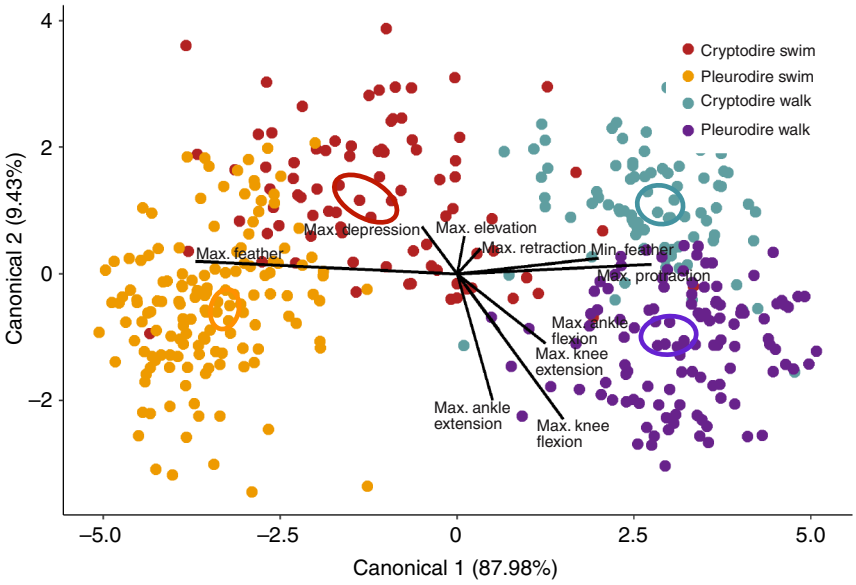

Fig. 7. Canonical discriminant function analysis of hindlimb kinematics in cryptodire (*T. scripta*) and pleurodire (*E. subglobosa*) turtles. Kinematics are defined primarily by the environment the animal is experiencing. Colors of points indicate different cycle categories: red, cryptodire swimming (*N*=84); yellow, pleurodire swimming (*N*=149); blue, cryptodire walking (*N*=88); purple, pleurodire walking (*N*=116). Colored ovals represent the 95% confidence limit for the mean of each of these four groups. Black lines indicate the magnitude and direction of the loading of each variable (Youngerman et al., 2014). Canonical 1 is defined by differences in swimming and walking, with increased feathering defining swimming, and greater protraction angles defining walking. Canonical 2 discriminates species, with pleurodires exhibiting decreased knee flexion and increased ankle extension.

might relate to the differences in leverage imposed by pelvic-shell fusion, other differences in hindlimb muscle activity and kinematics are likely independent of the structural differences between the two lineages. For example, knee kinematics (Fig. 6E,F) and FT muscle activity (Figs 4 and 5) differ substantially between pleurodires and cryptodires. These differences are apparent even though FT does not cross the hip, and its disposition is not affected by the presence or absence of pelvic-shell fusion. These results indicate that the substantial anatomical changes in the lever systems of turtle hindlimbs are not the only factor that may result in novel patterns of muscle use. Moreover, in the absence of structural changes, kinematic differences between groups can be expected to be driven by differences in motor pattern (Smith, 1994).

Overall, we found that species (pleurodire versus cryptodire) had the greatest influence in defining patterns of hindlimb muscle use in semiaquatic turtles (Fig. 5), whereas environment (water versus land) had the greatest influence in defining their patterns of kinematics (Fig. 7). With regard to muscle activity patterns, pleurodire walking differed from all other groups along the primary axis of variation in multivariate analyses, and pleurodire swimming separated from cryptodire walking and swimming along the second axis of variation (Fig. 5). In contrast, differences between walking and swimming explained the majority of kinematic variation in our sample, with some of the main features contributing to this distinction relating to variables that likely have little connection to differences in pelvic muscle moment arms between the groups (e.g. pedal feathering angle) (Fig. 7). Our multivariate results reinforce the dramatic kinematic differences required to produce effective locomotion between water and land in both species, regardless of differences in muscle use between species (Gillis and Blob, 2001; Nauwelaerts and Aerts, 2003; Rivera and Blob, 2010). Thus, changes in limb structure may relate to changes in limb muscle motor pattern and locomotor behavior in some cases, but these levels of variation also seem to show considerable independence (Smith, 1994; Lauder and Reilly, 1996).

Although not all differences in activity patterns between pleurodire and cryptodire hindlimb muscles were correlated with differences in muscle leverage, it is striking that for muscles that did differ in leverage between our focal taxa, pleurodires always showed greater normalized muscle moment arms than cryptodires (Table 1). This result makes a noteworthy parallel with Walker's (1973) comparisons of the shoulder muscles of a variety of turtle taxa, in which he found that the shoulder muscles of aquatic turtles exhibit greater mechanical advantage than those of their terrestrial relatives. Elevated moment arms may help habitually aquatic, limb-propelled swimmers to produce force-generating movements within the compliant environment of water.

In this context, it is notable that pleurodire turtles, including *E. subglobosa*, have remained a primarily aquatic lineage throughout their evolutionary history, whereas cryptodires have radiated onto land multiple independent times (Joyce and Gauthier, 2004; Bonin et al., 2006). In addition to being affected by differences in muscle attachment, muscle function also can be influenced by the external environment (Gillis and Blob, 2001; Nishikawa et al., 2007; Foster and Higham, 2017; Janshen et al., 2017), and animals often exhibit differences in both the timing (Gillis and Biewener, 2000; Blob et al., 2008) and intensity (Biewener and Gillis, 1999; Gillis and Biewener, 2000) of muscle use during locomotion in water and on land. In addition to structural variations, such as differences in muscle moment arms, such dynamic modulations of muscle activity are likely an important component of motor control that allows animals to use the same structures to move through different environments (Gillis, 1998; Earhart and Stein, 2000; Rivera et al., 2010; Ashley-Ross et al., 2014; Perlman and Ashley-Ross, 2016).

Finally, our data may also provide insight into aspects of the water-to-land transition in vertebrates. The capacity for performance in multiple environments may be facilitated because changes in limb function are not necessarily related to changes in limb structure (Gillis and Blob, 2001). As a result, the initial invasions of land may have proceeded with structures used in aquatic environments, with muscle use being modulated before structural changes occurred (Cole et al., 2011; Boisvert et al., 2013; Kawano and Blob, 2013; Horner and Jayne, 2014; McInroe et al., 2016).

Acknowledgements

We thank A. Arellanez, K. Diamond, J. Youngblood, A. Rubin, C. Petty and A. Sansone for assistance with surgeries and data collection, M. Sears and S. Kawano for their assistance with statistics, and two anonymous reviewers for their comments on the manuscript.

Competing interests

The authors declare no competing or financial interests.

Author contributions

Conceptualization: C.J.M., R.W.B.; Methodology: C.J.M., R.W.B.; Software: C.J.M., A.R.R., R.W.B.; Validation: C.J.M.; Formal analysis: C.J.M.; Investigation: C.J.M., J.E.P., M.N.S., R.W.B.; Resources: C.J.M., R.W.B.; Data curation: C.J.M.; Writing - original draft: C.J.M., J.E.P.; Writing - review & editing: C.J.M., J.E.P., M.N.S., A.R.R., R.W.B.; Visualization: C.J.M., M.N.S.; Supervision: C.J.M., R.W.B.; Project administration: C.J.M., R.W.B.; Funding acquisition: C.J.M., R.W.B.

Funding

This work was supported by a Sigma Xi grant to C.J.M., and Clemson University Creative Inquiry funds (grant 479) to R.W.B.

Data availability

Data are available from the Dryad Digital Repository (Mayerl et al., 2016): http://dx.doi.org/10.5061/dryad.8j413.

Supplementary information

Supplementary information available online at
http://jeb.biologists.org/lookup/doi/10.1242/jeb.157792.supplemental

References

Ahn, A. N. and Full, R. J. (2002). A motor and a brake: two leg extensor muscles acting at the same joint manage energy differently in a running insect. *J. Exp. Biol.* **205**, 379-389.

Aiello, B. R., Blob, R. W. and Butcher, M. T. (2013). Correlation of muscle function and bone strain in the hindlimb of the river cooter turtle (*Pseudemys concinna*). *J. Morphol.* **274**, 1060-1069.

Anderson, P. S. L. and Patek, S. N. (2015). Mechanical sensitivity reveals evolutionary dynamics of mechanical systems. *Proc. Biol. Sci. Lond. B.* **282**, 20143088.

Ashley-Ross, M. A., Perlman, B. M., Gibb, A. C. and Long, J. H.Jr (2014). Jumping sans legs: does elastic energy storage by the vertebral column power terrestrial jumps in bony fishes? *Zoology* **117**, 7-18.

Bates, D., Mäachler, M., Boker, B. and Walker, S. (2015). Fitting linear mixed-effects models using {lme4}. *J. Stat. Soft.* **67**, 1-48.

Biewener, A. A. (1989). Scaling body support in mammals: limb posture and muscle mechanics. *Science* **245**, 45-48.

Biewener, A. A. and Full, R. J. (1992). Force platform and kinematic analysis. In *Biomechanics – Structures and Systems: A Practical Approach* (ed. A. A. Biewener), pp. 45-73. New York, NY: Oxford University Press.

Biewener, A. A. and Gillis, G. B. (1999). Dynamics of muscle function during locomotion: accommodating variable conditions. *J. Exp. Biol.* **202**, 3387-3396.

Blob, R. W., Rivera, A. R. V. and Westneat, M. W. (2008). Hindlimb function in turtle locomotion: limb movements and muscular activation across taxa, environment, and ontogeny. In *Biology of Turtles* (ed. J. Wyneken, M. H. Godfery and V. Bels), pp. 139-162. Boca Raton, FL: CRC Press.

Boisvert, C. A., Joss, J. M. P. and Ahlberg, P. E. (2013). Comparative pelvic development of the axolotl (*Ambystoma mexicanum*) and the Australian lungfish (*Neoceratodus forsteri*): conservation and innovation across the fish–tetrapod transition. *Evodevo* **4**, 3.

Bonin, F., Devaux, B. and Dupré, A. (2006). *Turtles of the World*. Baltimore, MD: The Johns Hopkins University Press.

Cohen, J. (1992). A power primer. *Psychol. Bull.* **112**, 155-159.

Cole, N. J., Hall, T. E., Don, E. K., Berger, S., Boisvert, C. A., Neyt, C., Ericsson, R., Joss, J. M., Gurevich, D. B. and Currie, P. D. (2011). Development and evolution of the muscles of the pelvic fin. *PLoS Biol.* **9**, 16-18.

Dial, K. P., Goslow, G. E., Jr and Jenkins, F. A., Jr (1991). The functional anatomy of the shoulder girdle in the European starling (*Sturnus vulgaris*). *J. Morphol.* **207**, 327-344.

Earhart, G. M. and Stein, P. S. G. (2000). Step, swim, and scratch motor patterns in the turtle. *J. Neurophysiol.* **84**, 2181-2190.

Foster, K. L. and Higham, T. E. (2017). Integrating gastrocnemius force-length properties, *in vivo* activation and operating lengths reveals how *Anolis* deal with ecological challenges. *J. Exp. Biol.* **220**, 796-806.

Gillis, G. B. (1998). Environmental effects on undulatory locomotion in the American eel *Anguilla rostrata*: kinematics in water and on land. *J. Exp. Biol.* **201**, 949-961.

Gillis, G. B. and Biewener, A. A. (2000). Hindlimb extensor muscle function during jumping and swimming in the toad (*Bufo marinus*). *J. Exp. Biol.* **203**, 3547-3563.

Gillis, G. B. and Blob, R. W. (2001). How muscles accommodate movement in different physical environments: aquatic vs. terrestrial locomotion in vertebrates. *Comp. Biochem. Physiol. Part A* **131**, 61-75.

Hedrick, T. L. (2008). Software techniques for two- and three-dimensional kinematic measurements of biological and biomimetic systems. *Bioinspir. Biomim.* 3, 34001.

Horner, A. M. and Jayne, B. C. (2014). Lungfish axial muscle function and the vertebrate water to land transition. *PLoS ONE* **9**, e96516.

Hulsey, C. D., Roberts, R. J., Lin, A. S. P., Guldberg, R. and Streelman, J. T. (2008). Convergence in a mechanically complex phenotype: detecting structural adaptations for crushing in cichlid fish. *Evolution* **62**, 1587-1599.

Hutchinson, J. R., Anderson, F. C., Blemker, S. S. and Delp, S. L. (2005). Analysis of hindlimb muscle moment arms in *Tyrannosaurus rex* using a three-dimensional musculoskeletal computer model: implications for stance, gait, and speed. *Paleobiology* **31**, 676-701.

Janshen, L., Santuz, A., Ekizs, A. and Arampatzis, A. (2017). Modular control during incline and level walking in humans. *J. Exp. Biol.* **220**, 807-813.

Jenkins, F. A. and Goslow, G. E.Jr (1983). The functional anatomy of the shoulder of the savannah monitor lizard (*Varanus exanthematicus*). *J. Morphol.* **175**, 195-216.

Joyce, W. G. and Gauthier, J. A. (2004). Palaeoecology of Triassic stem turtles sheds new light on turtle origins. *Proc. R. Soc. Lond. B.* **271**, 1-5.

Kargo, W. J. and Rome, L. C. (2002). Functional morphology of proximal hindlimb muscles in the frog *Rana pipiens*. *J. Exp. Biol.* **205**, 1987-2004.

Kawano, S. M. and Blob, R. W. (2013). Propulsive forces of mudskipper fins and salamander limbs during terrestrial locomotion: implications for the invasion of land. *Integr. Comp. Biol.* **53**, 283-294.

Lauder, G. V. and Reilly, S. M. (1996). The mechanistic bases of behavioral evolution: a multivariate analysis of musculoskeletal function. In *Phylogenies and the Comparative Method in Animal Behavior* (ed. E. P. Martins), pp. 104-137. New York, NY: Oxford University Press.

Mayerl, C. J., Brainerd, E. L. and Blob, R. W. (2016). Pelvic girdle mobility of cryptodire and pleurodire turtles during walking and swimming. *J. Exp. Biol.* **219**, 2650-2658.

McInroe, B., Astley, H. C., Gong, C., Kawano, S. M., Schiebel, P. E., Rieser, J. M., Choset, H., Blob, R. W. and Goldman, D. I. (2016). Tail use improves performance on soft substrates in models of early vertebrate land locomotors. *Science* **353**, 154-158.

Nauwelaerts, S. and Aerts, P. (2003). Propulsive impulse as a covarying performance measure in the comparison of the kinematics of swimming and jumping in frogs. *J. Exp. Biol.* **206**, 4341-4351.

Nishikawa, K., Biewener, A. A., Aerts, P., Ahn, A. N., Chiel, H. J., Daley, M. A., Daniel, T. L., Full, R. J., Hale, M. E., Hedrick, T. L. et al. (2007). Neuromechanics: an integrative approach for understanding motor control. *Int. Comp. Biol.* **47**, 16-54.

Pace, C. M., Blob, R. W. and Westneat, M. W. (2001). Comparative kinematics of the forelimb during swimming in red-eared slider (*Trachemys scripta*) and spiny softshell (*Apalone spinifera*) turtles. *J. Exp. Biol.* **204**, 3261-3271.

Perlman, B. M. and Ashley-Ross, M. A. (2016). By land or by sea: a modified C-start motor pattern drives the terrestrial tail flip. *J. Exp. Biol.* **219**, 1860-1865.

Rivera, A. R. V. and Blob, R. W. (2010). Forelimb kinematics and motor patterns of the slider turtle (*Trachemys scripta*) during swimming and walking: shared and novel strategies for meeting locomotor demands of water and land. *J. Exp. Biol.* **213**, 3515-3526.

Rivera, A. R. V., Wyneken, J. and Blob, R. W. (2011). Forelimb kinematics and motor patterns of swimming loggerhead sea turtles (*Caretta caretta*): are motor patterns conserved in the evolution of new locomotor strategies? *J. Exp. Biol.* **214**, 3314-3323.

Roberts, T. J., Marsh, R. L., Weyand, P. G. and Taylor, C. R. (1997). Muscular force in running turkeys: the economy of minimizing work. *Science* **275**, 1113-1115.

Smith, K. K. (1994). Are neuromotor systems conserved in evolution? *Brain. Behav. Evol.* **43**, 293-305.

Smith, J. M. and Savage, R. J. G. (1956). Some locomotory adaptations in mammals. *J. Linn. Soc. Lond. Zool.* **42**, 603-622.

Venables, W. N. and Ripley, B. D. (2002). *Modern applied statistics with S*. 4th edn. New York, NY: Springer.

Vogel, S. (2013). *Comparative Biomechanics: Life's Physical World*. Princeton, NJ: Princeton University Press.

Wainwright, P. C. and Lauder, G. V. (1986). Feeding biology of sunfishes: patterns of variation in the feeding mechanism. *Zool. J. Linn. Soc.* **88**, 217-228.

Walker, W. F., Jr (1973). The locomotor apparatus of testudines. In *Biology of the Reptilia*. Vol. IV. Morphology, part D (ed. C. Gans and T. S. Parsons), pp. 1-100. New York: Academic Press.

Westneat, M. W. (1994). Transmission of force and velocity in the feeding mechanisms of labrid fishes (Teleostei, Perciformes). *Zoomorphology* **114**, 103-118.

Westneat, M. W. and Wainwright, P. C. (1989). Feeding mechanism of *Epibulus insidiator* (Labridae; Teleostei): Evolution of a novel functional system. *J. Morphol.* **202**, 129-150.

Xu, R. (2003). Measuring explained variation in linear mixed effects models. *Stat. Med.* **22**, 3527-3541.

Youngerman, E. D., Flammang, B. E. and Lauder, G. V. (2014). Locomotion of free-swimming ghost knifefish: anal fin kinematics during four behaviors. *Zoology* **117**, 337-348.

Zug, G. (1971). Buoyancy, locomotion, morphology of the pelvic girdle and hindlimb, and systematics of cryptodiran turtles. *Misc. Publ. Mus. Zool. Univ. Michigan* **142**, 1-104.

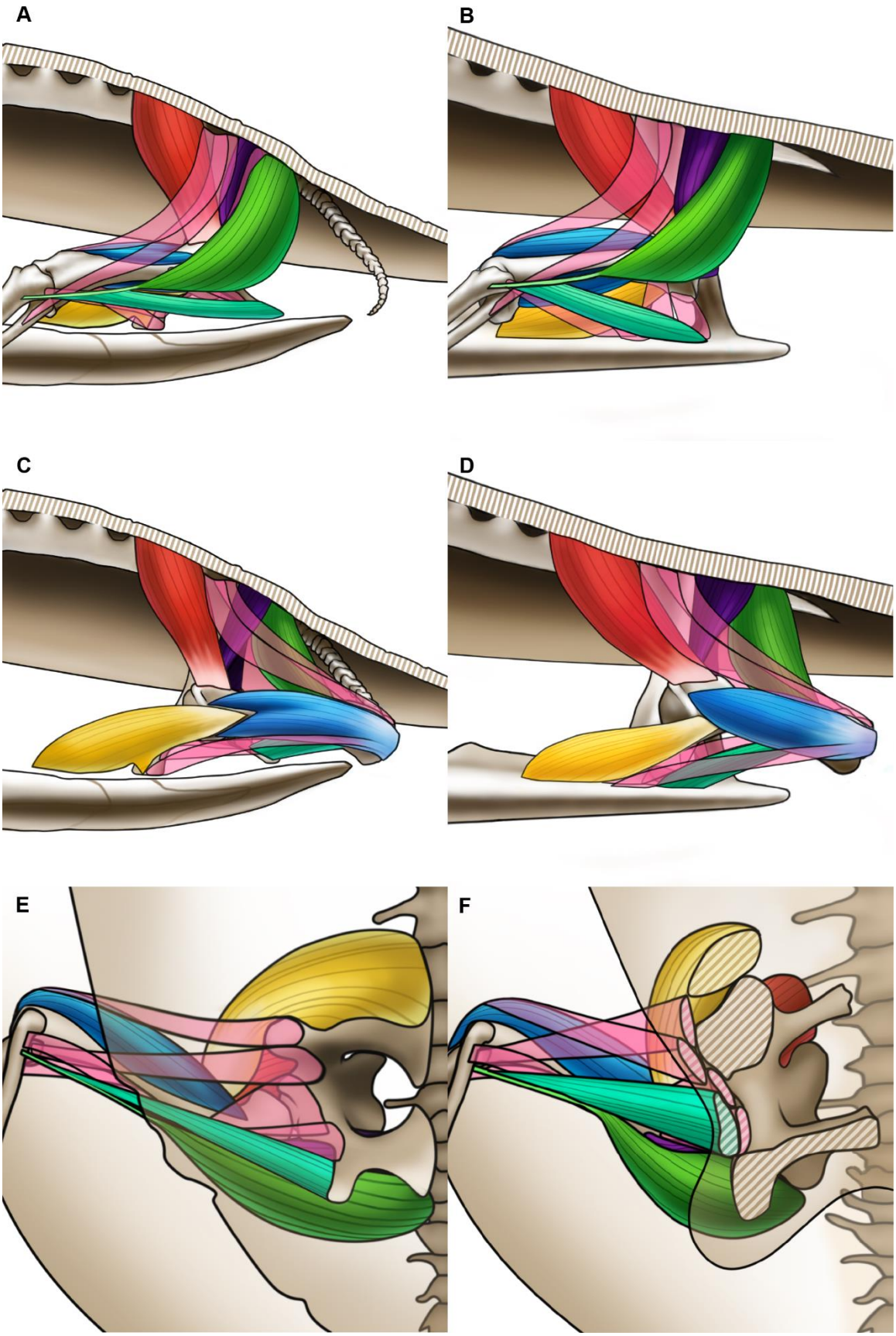

Figure S1. **Illustrations of all hindlimb muscles in the cryptodire *T. scripta* (left) and the pleurodire *E. subglobosa* (right) which have shifted from the ancestral origin on the pelvis in cryptodires to an origin on the shell in pleurodires**. A,B lateral view with femur protracted, anterior is on the left; C,D lateral view with femur retracted, anterior is on the left; E,F ventral view with femur protracted, anterior is to the top. Hatched areas in F indicate the attachment of the pelvis and muscles to the shell. Yellow, Puboischiofemoralis internus (PIFI); Red, Iliofemoralis (ILF); Blue, Femorotibialis (FT); Green, Flexor tibialis internus (FTI); Purple, Caudi-iliofemoralis (CIF). Pink muscles are those not examined in this study. A-D, Dorsal muscles, Iliotibialis (anterior), Iliofibularis (posterior). E,F, Ventral muscles, anterior to posterior, ambiens, pubo-tibialis, adductor femoris, ischiotrochantericus.

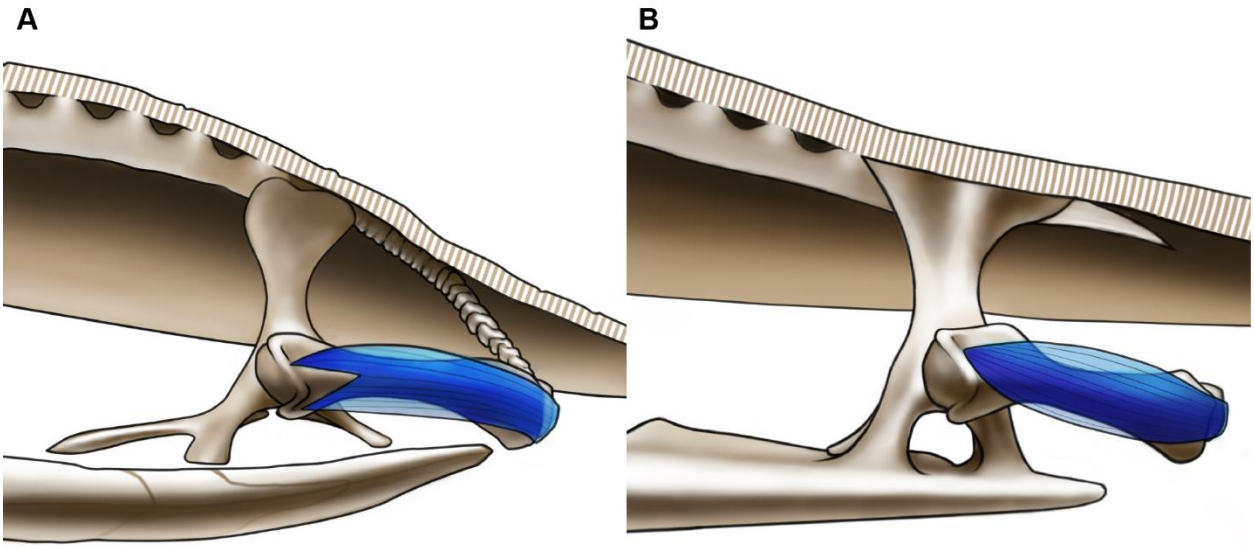

Figure S2. **Isolated femorotibialis muscle (blue) in the cryptodire *T. scripta* (A) and pleurodire *E. globosa* (B)**. This muscle is not associated with the hip joint, and demonstrates no substantial change in muscle origin between the two lineages.

Table S1: Hindlimb muscle use data collected from cryptodire and pleurodire turtles while swimming and walking.

Muscle	Swimming		Walking	
	Cryptodire	Pleurodire	Cryptodire	Pleurodire
PIFI	3, 44	3, 74	2, 32	3, 66
ILF	3, 48	3, 40	3, 47	1, 23
FT	3, 51	1, 28	3, 51	1, 26
FTI	3, 50	3, 69	3, 43	3, 78
CIF	2, 33	3, 65	2, 36	3, 43

Numbers for each lineage indicate sample sizes for each muscle during each behavior (individuals, cycles). PIFI, puboischiofemoralis internus; ILF, iliofemoralis; FT, femorotibialis; FTI, flexor tibialis internus; CIF, caudi-iliofemoralis.

Table S2. Muscle activity patterns during locomotion while swimming and walking in cryptodire and pleurodire turtles.

		Swim		Walk			
Muscle	Action	Cryptodire	Pleurodire	Cryptodire	Pleurodire	Canon 1	Canon 2
PIFI	On	43.08 ± 1.38	48.35 ± 0.45	53.12 ± 1.22	77.96 ± 0.73	0.41	-0.26
	Off	82.80 ± 0.83	89.23 ± 0.27	86.53 ± 1.01	101.76 ± 0.32	0.40	0.30
ILF	On	35.37 ± 1.21	55.18 ± 1.76	46.83 ± 1.20	76.57 ± 0.99	0.14	-0.07
	Off	65.09 ± 1.07	84.11 ± 1.52	74.83 ± 1.27	98.35 ± 0.47	0.46	0.29
FT	On			5.24 ± 0.97	31.87 ± 1.85		
stance	Off			38.54 ± 1.01	51.58 ± 1.43		
FT	On	75.05 ± 0.74	82.58 ± 0.75	84.18 ± 0.60	87.59 ± 0.82	0.33	-0.39
swing	Off	91.25 ± 0.65	104.02 ± 0.72	93.95 ± 0.60	99.62 ± 0.26	0.06	0.97
FTI	On	-3.38 ± 0.74	-0.96 ± 0.66	-0.71 ± 0.86	0.49 ± 0.36	-0.22	0.05
	Off	22.29 ± 1.21	18.43 ± 1.13	28.50 ± 0.93	53.60 ± 1.16	0.54	-0.12
CIF	On	-4.23 ± 0.73	1.82 ± 0.50	-0.14 ± 0.39	1.50 ± 0.60	0.07	0.46
	Off	19.94 ± 1.26	22.27 ± 0.61	30.73 ± 0.89	47.35 ± 1.48	0.41	-0.48

Values are mean ± SE activity timing (in percentage of limb cycle, with 0 when the limb is fully protracted). Canonical values are loaded scores for each variable in the CDA. PIFI, puboischiofemoralis internus; ILF, iliofemoralis; FT, femorotibialis; FTI, flexor tibialis internus; CIF, caudi-iliofemoralis.

Table S3. Kinematics of cryptodire and pleurodire turtles, with p values, overall effects size (Ω^2), effects size of species (Cohen's d) for each environment, as well as the canonical discriminant loadings for the overall data.

	Swimming					Walking					Canon	Canon
	Cryptodire	**Pleurodire**	**p**	**Ω^2**	**D**	**Cryptodire**	**Pleurodire**	**p**	**Ω^2**	**D**	**1**	**2**
Max Pro	63.4 ± 0.8	47.1 ± 0.5	<0.001	0.861	2.333	69.6 ± 0.5	64.2 ± 0.7	0.094	0.842	0.867	0.83	0.05
Max Ret	-11.4 ± 1.9	-26.6 ± 0.6	0.005	0.682	1.254	-1.4 ± 2.7	-13.2 ± 1.4	0.234	0.728	0.578	0.13	0.16
Max El	-4.7 ± 0.6	-10.8 ± 0.6	0.029	0.710	0.949	-1.4 ± 0.4	-7.9 ± 0.4	<0.001	0.685	1.646	0.05	0.25
Max Dep	-21.3 ± 0.7	-28.1 ± 0.7	0.136	0.750	0.839	-18.8 ± 0.4	-26.0 ± 0.5	0.003	0.772	1.509	-0.18	0.31
Knee Ext	109.4 ± 1.5	130.7 ± 1.0	0.001	0.805	-1.658	107.5 ± 2.3	121.6 ± 1.5	0.171	0.806	0.748	0.36	-0.33
Knee Flex	50.7 ± 1.0	64.8 ± 1.2	0.003	0.801	-1.177	49.7 ± 1.5	66.9 ± 1.6	0.068	0.888	-1.067	0.50	-0.67
Ankle Ext	81.6 ± 1.5	80.1 ± 1.2	0.382	0.688	0.100	93.5 ± 2.5	96.9 ± 2.1	0.877	0.695	-0.155	0.35	-0.58
Ankle Flex	30.6 ± 1.4	19.5 ± 1.2	0.402	0.879	0.781	34.1 ± 1.6	41.9 ± 1.9	0.428	0.708	-0.436	0.18	-0.26
Max Feath	67.3 ± 2.3	85.4 ± 1.2	0.004	0.757	-1.059	27.0 ± 1.3	25.2 ± 1.4	0.998	0.690	0.125	-1.18	0.05
Min Feath	-0.4 ± 2.2	3.6 ± 1.3	0.343	0.622	-0.226	-4.9 ± 1.3	-9.7 ± 0.6	0.622	0.743	0.338	0.62	0.11

Values are mean angles ± SE. p values reported are those from mixed effects models, Ω^2 provides an effects size for the overall model, and D represents the Cohen's d value for the main effect in the model (species). N = 5 individuals, 84 cycles for cryptodire swimming, and 88 cycles for cryptodire walking; N = 6 individuals, 149 cycles for pleurodire swimming, and 116 cycles for pleurodire walking. Max Pro, Maximum protraction; Max Ret, maximum retraction; Max El, Maximum elevation; Max dep, Maximum depression; Knee Ext, Maximum knee extension; Knee Flex, Maximum knee flexion; Ankle Ext, maximum ankle extention; Ankle Flex, maximum ankle flexion; Max Feath, Maximum angle of pes; Min Feath, minimum angle of pes.